

# EXERGY STUDY OF THE KALINA CYCLE

Göran Wall

University College of Eskilstuna/Västerås, Box 11, S-721 03 Västerås, Sweden.

and

Chia-Chin Chuang and Masaru Ishida

Tokyo Institute of Technology, Research Laboratory of Resources Utilization  
4259 Nagatsuta, Midori-ku, Yokohama, 227 Japan

*presented at*

1989 American Society of Mechanical Engineers (ASME), Winter Annual Meeting (WAM)  
San Francisco, California  
December 10-15, 1989

*published in*

R. A. Bajura, M. R. von Spakovsky and E. S. Geskin Eds., *Analysis and Design of Energy Systems: Analysis of Industrial Processes*, AES-Vol. 10-3, pp. 73-77, ASME.

**Abstract**—Energy-Utilization Diagrams is a graphic method to describe the exergy losses in industrial processes, i.e., improving the exergy use. We apply the method to a 3MW Kalina bottoming cycle. The Kalina cycle is being developed as a competitive improvement of the Rankine steam cycle. By using an ammonia-water mixture as the working fluid and a condensing system based on absorption refrigeration principles the Kalina bottoming cycle becomes about 10% more efficient than the ordinary Rankine cycle. The Energy-Utilization Diagram of the Kalina cycle is very tight. From this we see that the cycle is very well optimized.

## NOMENCLATURE

- $c$  Specific heat
- $e$  Exergy per unit mass
- $g$  Gibbs free energy per unit mass
- $h$  Enthalpy per unit mass
- $p$  Pressure;  $p_c$  critical pressure
- $R$  Gas constant;  $R_m$  for mixture
- $s$  Entropy per unit mass
- $T$  Temperature;  $T_b$  bubble point;  $T_d$  dew point;  $T_c$  critical point;  $T_s$  saturation point for a pure component
- $u$  Energy per unit mass
- $v$  Volume per unit mass
- $X$  Ammonia mass fraction;  $X_m$  for ammonia mol fraction
- $\rho$  Density

## Subscripts

- $f$  Saturated liquid
- $g$  Saturated vapor
- $l$  Subcooled liquid
- $m$  Mixture or mol fraction
- $v$  Superheated vapor
- $s$  Saturation
- $sol$  Solution
- Ideal gas

INTRODUCTION

Energy-Utilization Diagrams (EUD) is an important engineering tool to improve exergy efficiency of energy conversion systems (Ishida and Zheng, 1986 and Ishida et al., 1987). The exergy losses of the system are shown by a graphical presentation which gives a useful overall description of the process.

The use of mixtures as working fluids has opened new possibilities to improve the efficiency of power and refrigeration cycles with less costly equipment. Mixtures may be an important substitute for CFC refrigerants, thus, decreasing environmental problems. The Kalina cycle, which use a ammonia-water mixture, may show 10 to 20% higher exergy efficiency than the conventional Rankine cycle (Kalina, 1984 and El-Sayed and Tribus, 1985). The ammonia-water mixture boils at a variable temperature unlike pure water which boils at a constant temperature. Variable temperature boiling permits the working fluid to maintain a temperature closer to that of the hot combustion gases in the boiler, thus, improving the exergy efficiency, a fact which has been well known among scientist and engineers. But there was no practical, efficient way to condense the mixture back to a fluid for recycling until the Kalina cycle was introduced.

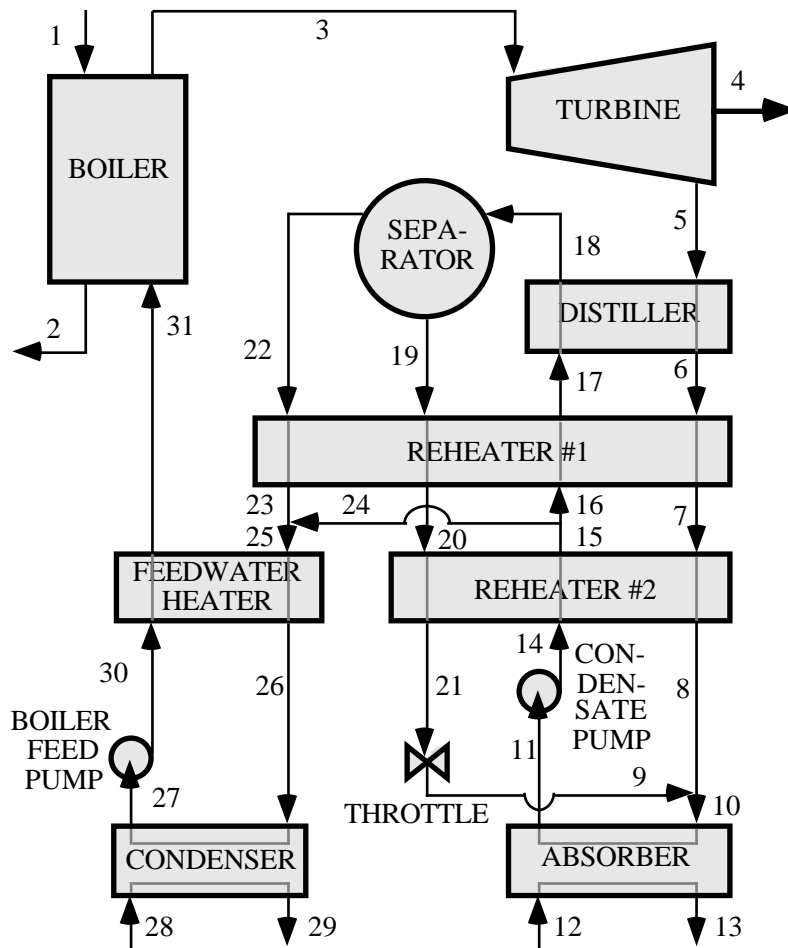


Figure 1. A simplified Kalina cycle

By circulating the mixture at different compositions in different parts of the cycle, condensation (absorption) can be done at slightly above atmospheric pressure with a low concentration of ammonia, while heat input is at a higher concentration for optimum cycle performance.

Figure 1 shows the simplified Kalina cycle (El-Sayed and Tribus, 1985a) assumed in this study. This is a bottoming cycle feed by exhaust gases (1, 2) to the boiler. Superheated

ammonia-water vapor (3) is expanded in a turbine to generate work (4). The turbine exhaust (5) is cooled (6, 7, 8), diluted with ammonia-poor liquid (9, 10) and condensed (11) in the absorber by cooling water (12, 13). The saturated liquid leaving the absorber is compressed (14) to an intermediate pressure and heated (15, 16, 17, 18). The saturated mixture is separated into an ammonia-poor liquid (19) which is cooled (20, 21) and depressurized in a throttle and ammonia-rich vapor (22) is cooled (23) and some of the original condensate (24) is added to the nearly pure ammonia vapor to obtain an ammonia concentration of about 70% in the working fluid (25). The mixture is then cooled (26), condensed (27) by cooling water (28, 29), compressed (30), and sent to the boiler via regenerative feedwater heater (31).

The mass flow circulating between the separator and the absorber is about 4 times that of the turbine, thus, causing some additional condensate pump work. However, this loop makes possible the changes in composition between initial condensation in the absorber and heat addition in the boiler. By changing the dew point of the mixture, the waste heat from the turbine exhaust, which is lost in a Rankine cycle, can be used to dilute the ammonia-water vapor with a stream of water, thus, producing a mixture with a substantially lower concentration of ammonia which allows condensation at a much higher temperature.

Usually thermodynamic properties of pure fluids and information of the departure from ideal-solution is sufficient to derive mixture properties. Stability, secondary reactions, safety, etc must, of course, also be considered.

## ENERGY-UTILIZATION DIAGRAMS

In the present method, it is assumed that a system is composed of a number of subsystems containing energy-donating and energy-accepting processes.

Let us consider the processes in a subsystem. The first law of thermodynamics states that the total energy is conserved, i.e.:

$$H_k = 0 \quad (k = 1, \dots, \hat{k}), \quad (1)$$

where  $\hat{k}$  is the number of processes in the subsystem. Classified into energy donors and energy acceptors, the above equation becomes

$$H_k^{\text{ed}} + H_k^{\text{ea}} = 0, \quad (2)$$

where the superscript ed and ea mean energy donor and energy acceptor, respectively.

The second law of thermodynamics states that the total entropy is increased:

$$S_k = S_k^{\text{ed}} + S_k^{\text{ea}} \geq 0. \quad (3)$$

Then exergy is lost in the process system:

$$E_k = H_k - T_0 S_k = -T_0 (S_k^{\text{ed}} + S_k^{\text{ea}}) \leq 0. \quad (4)$$

If we introduce the availability factor  $A$  (M. Ishida and K. Kawamura, 1982),

$$A = E / H, \quad (5)$$

equation 4 may be converted to:

$$-E_k = H_k^{\text{ea}} (A_k^{\text{ed}} - A_k^{\text{ea}}). \quad (6)$$

When  $\hat{k}$  goes to infinity the relation becomes:

$$-dE = (A^{ed} - A^{ea})dH^{ea}. \quad (7)$$

Hence, by plotting  $A^{ed}$  and  $A^{ea}$  against  $H^{ea}$ , the exergy loss in the subsystem is represented by the area between  $A^{ed}$  and  $A^{ea}$ . This we call Energy-Utilization Diagrams.

## KALINA CYCLE

A simple model is assumed for the thermodynamic properties of the ammonia-water mixture used in the Kalina cycle. In the gas phase, above the saturation temperature of water  $T_{sw}$ , the superheated mixture is assumed to behave as an ideal solution of superheated ammonia and water vapor (fig. 2). When the temperature is between the pure water saturation temperature  $T_{sw}$  and the mixture dew point  $T_d$  in the gas phase, the water component is assumed in a meta-stable vapor state at the considered pressure. Similarly, in the liquid region, between the saturation temperature of pure ammonia  $T_{sa}$  and the bubble point of the mixture  $T_b$  we assume a meta-stable liquid state for ammonia. In the wet vapor mixture region  $T_d > T > T_b$  we have a saturated vapor mixture with ammonia mass fraction  $X_g$  and a saturated liquid mixture with ammonia mass fraction  $X_f$ . In the liquid region, below the bubble point of the mixture  $T_b$ , a Gibbs excess function for the departure from ideal-solution behavior is assumed (Kalina et al., 1986).

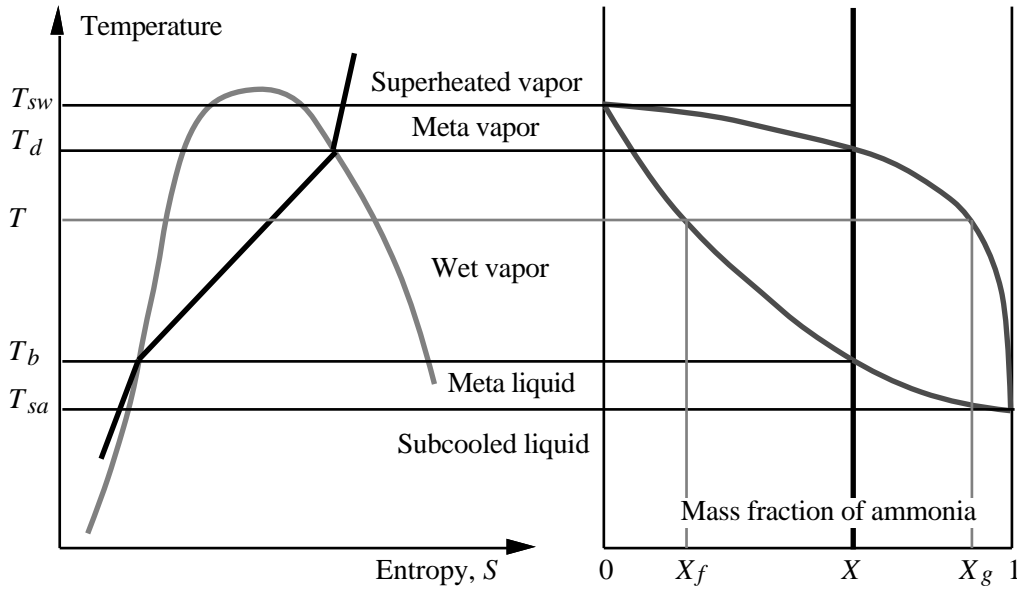


Figure 2. The various states on  $T$ - $S$  and  $T$ - $X$  diagrams.

## COMPUTATIONAL PROCEDURE

From the assumptions above the following thermodynamic properties are needed.

(1) Pure ammonia and water:

$$p = p(\rho, T) \quad (8)$$

$$c_v = c(T) \quad (9)$$

$$\rho_f = \rho(T_{sat}) \quad (10)$$

$$p_{sat} = p(T_{sat}) \quad (11)$$

$$(dp/dT)_{sat} = h_{fg}/(T v_{fg}) \quad (12)$$

The properties of the pure components are available in tables or by equations (Haar and Gallagher, 1978 and Keenan et al., 1969), and a compilation of 40 substances by Reynolds was used (1980). Energy, entropy, enthalpy, and exergy per unit mass are calculated using Eqs. 8 and 9 and the following thermodynamic relations:

$$u = u_0 + \int_0^T c_v dT + \int_0^{\rho} \frac{1}{\rho^2} (p - T \frac{p}{T \rho}) d\rho \quad (13)$$

$$s = s_0 + \int_0^T c_v /T dT + \int_0^{\rho} \frac{1}{\rho^2} (\rho R - \frac{p}{T \rho}) d\rho - R \ln \rho \quad (14)$$

$$h = u + pv \quad (15)$$

$$e = h - T_0 s \quad (16)$$

where  $u_0$  and  $s_0$  are chosen such that a selected reference state have a zero energy and enthalpy for pure saturated liquids at  $T_0 = 0^\circ\text{C}$ .

(2) Mixture of ammonia and water:

$$\text{Bubble point} \quad T_b = T(p, X) \quad (17)$$

$$\text{Dew point} \quad T_d = T(p, X) \quad (18)$$

$$\text{Gibbs free energy of solution} \quad g_{sol} = g(p, T, X) \quad (19)$$

Data for these equations are presented by El-Sayed and Tribus (1985b).

We may now develop relations for the ammonia-water mixture in the different regions defined in Fig. 2.

( $T > T_{sw}$ ) Superheated vapor:

$$h_{vm} = X h_{va} + (1 - X) h_{vw} \quad (20)$$

$$s_{vm} = X s_{va} + (1 - X) s_{vw} - R_m (X_m \ln X_m + (1 - X_m) \ln(1 - X_m)) \quad (21)$$

$$v_{vm} = X v_{va} + (1 - X) v_{vw} \quad (22)$$

( $T_{sw} > T > T_d$ ) Meta vapor: Eqs. 23-27 below were applied with Eqs. 20-22 above.

$$\text{Meta vapor water} \quad h_{vw} = h_{gw} - \tilde{c}_{pw} T \quad (23)$$

$$s_{vw} = s_{gw} - \tilde{c}_{pw} \ln(T_{sw}/T) \quad (24)$$

$$v_{vw} = v_{gw} (T/T_{sw}) \quad (25)$$

$$\text{where} \quad T = T_{sw} - T, \quad (26)$$

$$\text{and} \quad \tilde{c}_{pw} = (h_{vw} \text{ (at } T_{sw} + T) - h_{gw}) / T. \quad (27)$$

( $T_d > T > T_b$ ) Wet vapor: According to Fig. 2, a saturated vapor mixture with ammonia mass fraction  $X_g$  and a saturated liquid mixture with  $X_f$  occur. For the saturated vapor we apply the equations above and for the saturated liquid we use the following equations.

$$\text{Meta liquid ammonia} \quad h_{la} = h_{fa} + \tilde{c}_{pa} T \quad (28)$$

$$s_{la} = s_{fa} + \tilde{c}_{pa} \ln(T/T_{sa}) \quad (29)$$

$$v_{la} = v_{fa} \quad (30)$$

$$\text{where} \quad T = T - T_{sap} \quad (31)$$

$$\text{and} \quad \tilde{c}_{pa} = (h_{fa} - h_{la} \text{ (at } T_{sa} - T)) / T. \quad (32)$$

$$\text{Saturated liquid mixture} \quad h_{lm} = Xh_{la} + (1 - X)h_{lw} + h_{sol} \quad (33)$$

$$s_{lm} = Xs_{la} + (1 - X)s_{lw} - R_m(X_m \ln X_m + (1 - X_m) \ln(1 - X_m)) + s_{sol} \quad (34)$$

$$v_{lm} = Xv_{la} + (1 - X)v_{lw} + v_{sol} \quad (35)$$

$$\text{where} \quad h_{sol} = -T^2 (g_{sol}/T) / T, \quad (36)$$

$$s_{sol} = (h_{sol} - g_{sol})/T, \quad (37)$$

$$\text{and} \quad v_{sol} = g_{sol} / p. \quad (38)$$

( $T_b > T > T_{sa}$ ) Meta liquid: Eqs. 28-38 above were applied.

( $T_{sa} > T$ ) Subcooled liquid: Eqs. 33-38 above were applied.

The following equations were also used

$$\text{Clapeyrons equation} \quad h_{fg} = (v_g - v_f)T_s (p / T)_s \quad (39)$$

$$\text{and} \quad s_{fg} = h_{fg}/T_s \quad (40)$$

A computer algorithm based on these relations has been developed in Pascal to run on a microcomputer (Macintosh™).

## ENERGY-UTILIZATION DIAGRAM OF THE KALINA CYCLE

Figure 3 shows the Energy-Utilization Diagram for the Kalina cycle presented above. This diagram shows the scheme of energy transformations by plotting the amount of energy transformed on the abscissa (i.e., coordinate for the first law of thermodynamics) and the energy levels of the donor process ( $A^{ed}$ ) and the acceptor process ( $A^{ea}$ ) on the ordinate (i.e., coordinate for the second law).

It is found that there are pinches at several points. Hence, it is not so easy to operate the system and much attention should be paid especially to these pinches. However, when this is solved, the uniform distribution of exergy loss shows that this system is well-optimized.

The diagram is divided into different parts related to the components of the Kalina cycle in Fig. 1. This figure clearly shows whether the quality of the energy, i.e., exergy, supplied is sufficient and the level of excess. The total exergy loss in each subsystem is

shown as the area between the energy donating and energy accepting lines. (The shadowed area.) In the boiler exergy from the exhaust gases, the energy donating line is curved downwards, is transferred to the ammonia-water mixture, where we can see the part indicating variable temperature boiling in the middle of the energy accepting line. For the turbine gas expansion is the energy donor and its energy level becomes greater than unity, while a work sink with  $A = 1$  is the energy acceptor. The area between these two energy levels gives the exergy loss in the turbine and the work generated is obtained as the width of  $H^{ea}$ . The remaining part of the diagram shows the heat exchange in the remaining subsystems indicating a very well optimized system.

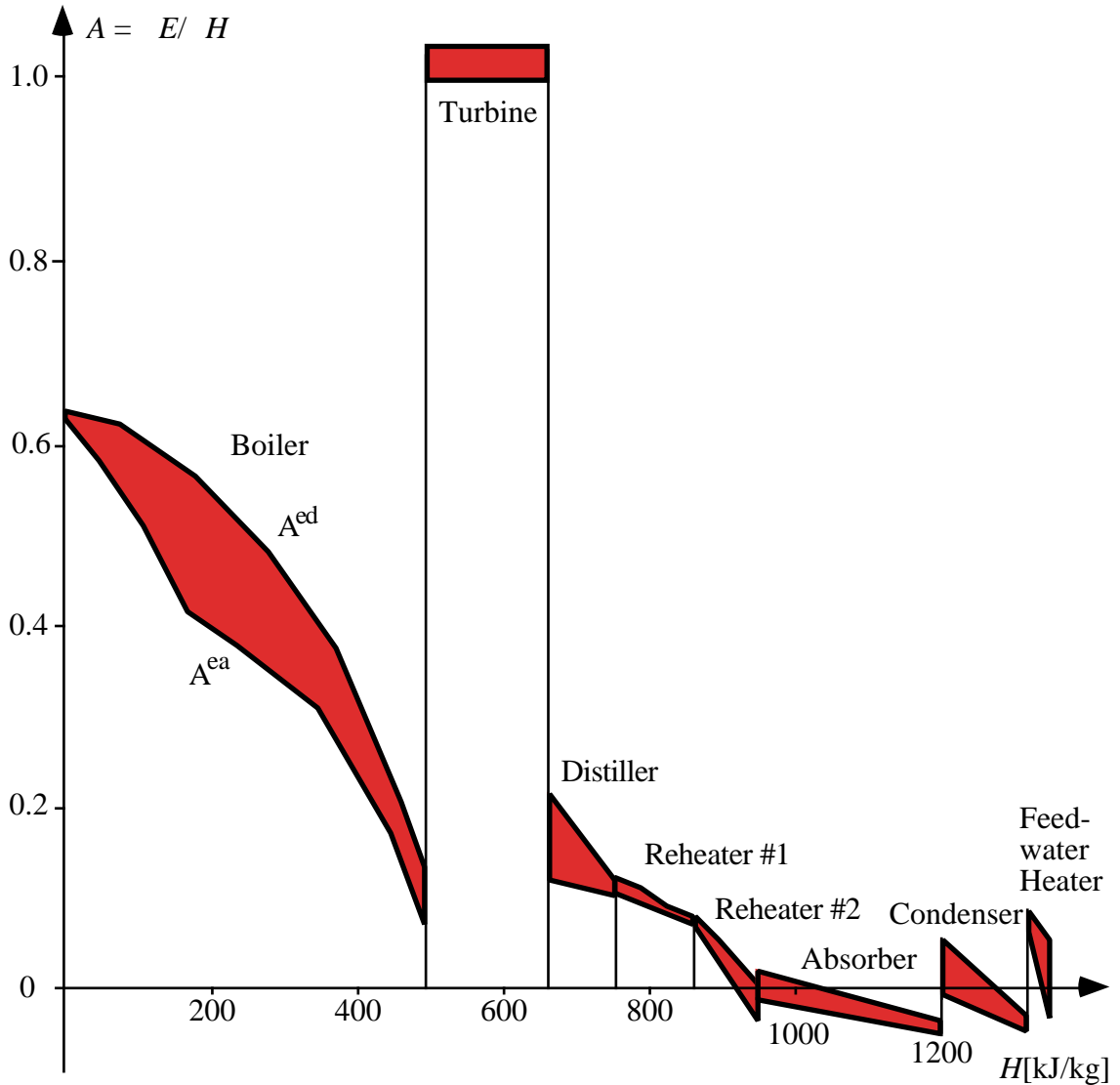


Figure 3. Energy-Utilization Diagram for the Kalina cycle.

## CONCLUSIONS

The characteristics of energy transformations in the Kalina cycle has been clarified through the use of Energy-Utilization Diagram which shows that the Kalina cycle is very well optimized. It is also found that the method of Energy-Utilization Diagrams effectively illustrates the internal phenomena by showing the distribution of exergy losses for each energy transformation. The exergy loss in the boiler is the highest among all subsystems but from the diagram we also see that to suggest improvements further studies are needed.

## REFERENCES

El-Sayed, Y. M. and Tribus, M., 1985a, "A Theoretical Comparison of the Rankine and Kalina Cycle", ASME publication AES-Vol. 1.

El-Sayed, Y. M. and Tribus, M., 1985b, "Thermodynamic Properties of Water-Ammonia Mixtures Theoretical Implementation for Use in Power Cycles Analysis", ASME publication AES-Vol. 1, 1985.

Haar, L. and Gallagher, J. S., 1978, "Thermodynamic Properties of Ammonia", *J. Phys. Chem. Ref. Data*, vol. 7, no. 30, pp. 635-792.

Ishida, M. and Kawamura, K., 1982, *Ind. Engng Chem., Process Des. Dev.* **21**, 690.

Ishida, M. and Zheng, D., 1986, "Graphic exergy analysis of chemical process systems by a graphic simulator, GSCHMER", *Computers and Chem. Eng.*, vol. 10, no. 6, pp. 525-532.

Ishida, M., Zheng, D., and Akehata, T., 1987, "Evaluation of chemical-looping-combustion power-generation system by graphic exergy analysis", *Energy*, vol. 12, no. 2, pp. 147-154.

Kalina, A. L., 1984, "Combined Cycle System with Novel Bottoming Cycle", *ASME Journal of Engineering for Power*, vol. 106, no. 4, Oct. 1984, pp. 737-742 or ASME 84-GT-135, Amsterdam.

Kalina, A. L., Tribus, M., and El-Sayed, Y. M., 1986, "A Theoretical Approach to the Thermophysical Properties of Two-Miscible-Component Mixtures For the Purpose of Power-Cycle Analysis", presented at the Winter Annual Meeting, ASME, Anaheim, California, December 7-12, publ. no. 86-WA/HT-54.

Keenan, J. H., Keyes, F. G., Hill, P. C., and Moore, J. G., 1969, *Steam Tables*, John Wiley and Sons, Inc., New York.

Reynolds, W. C., 1980, *Thermodynamic Properties in SI – graphs, tables and computational equations for 40 substances*, Department of Mechanical Engineering, Stanford University, Stanford, CA 94305.